The EMBO Journal Vol. 20 No. 7 pp. 1583–1592, 2001

GPI anchoring leads to sphingolipid-dependent retention of endocytosed proteins in the recycling endosomal compartment

Samit Chatterjee, Elizabeth R.Smith[1], Kentaro Hanada[2], Victoria L.Stevens[1] and Satyajit Mayor[3]

National Center for Biological Sciences, UAS-GKVK Campus, Bellary Road, Bangalore 560 065, India, [1]Department of Radiation Oncology, Emory University, Atlanta, GA, USA and [2]National Institute of Infectious Diseases, Toyama, Shinjuku-ku, Tokyo, Japan

[3]Corresponding author
e-mail: mayor@ncbs.res.in

Glycosylphosphatidylinositol (GPI) anchoring is important for the function of several proteins in the context of their membrane trafficking pathways. We have shown previously that endocytosed GPI-anchored proteins (GPI-APs) are recycled to the plasma membrane three times more slowly than other membrane components. Recently, we found that GPI-APs are delivered to endocytic organelles, devoid of markers of the clathrin-mediated pathway, prior to their delivery to a common recycling endosomal compartment (REC). Here we show that the rate-limiting step in the recycling of GPI-APs is their slow exit from the REC; replacement of the GPI anchor with a transmembrane protein sequence abolishes retention in this compartment. Depletion of endogenous sphingolipid levels using sphingolipid synthesis inhibitors or in a sphingolipid-synthesis mutant cell line specifically enhances the rate of endocytic recycling of GPI-APs to that of other membrane components. We have shown previously that endocytic retention of GPI-APs is also relieved by cholesterol depletion. These findings strongly suggest that functional retention of GPI-APs in the REC occurs via their association with sphingolipid and cholesterol-enriched sorting platforms or 'rafts'.

Keywords: endocytosis/GPI-anchored proteins/rafts/sorting/sphingolipids

Introduction

Glycosylphosphatidylinositol-anchored proteins (GPI-APs) are a large class of functionally diverse proteins that share an evolutionarily conserved C-terminal post-translational lipid modification, the GPI moiety (McConville and Ferguson, 1993). Besides acting as the sole means of anchorage for these proteins at the extracellular leaflet of the plasma membrane, this modification appears to be responsible for GPI-APs being apically targeted in polarized epithelia, and for transducing signals across bilayers (for review see Lisanti *et al*., 1990; Ferguson, 1994; Robinson, 1997).

GPI-APs appear to be internalized via a non-clathrin-mediated endocytic route (Bamezai *et al*., 1992; Keller *et al*., 1992; Ricci *et al*., 2000; Sabharanjak and Mayor, 1999; Skretting *et al*., 1999). We have found recently that they are delivered to peripheral tubular-vesicular endosomes called GEECs (GPI-AP enriched endosomal compartments), devoid of markers of the clathrin-mediated pathway (Sabharanjak and Mayor, 1999; S.Sabharanjak and S.Mayor, in preparation). These endosomal organelles, which contain a significant fraction of internalized fluid phase, deliver GPI-APs to the pericentriolar recycling endosomal compartment (REC). GPI-APs are not delivered to late endosomes, consistent with observations made in earlier studies (Kamen *et al*., 1988; Keller *et al*., 1992; Rijnboutt *et al*., 1996; Mayor *et al*., 1998). In the well characterized clathrin-mediated endocytic pathway, endocytosed molecules are delivered to sorting endosomes and then traffic to the REC or late endosomes (Gruenberg and Maxfield, 1995; Mukherjee *et al*., 1997).

After reaching the REC, recycling to the cell surface does not seem to be mediated by any specific signal: transferrin receptor (TfR), N-terminally truncated TfR lacking its cytoplasmic tail (δ3–59TfR) (Johnson *et al*., 1993; Marsh *et al*., 1995) and a fluorescent lipid inserted in the exoplasmic leaflet of the plasma membrane (Mayor *et al*., 1993) are recycled to the cell surface at a similar rate. However, GPI-APs recycle to the cell surface three to four times more slowly ($t_{1/2}$ ~30 min) than other components of the recycled membrane ($t_{1/2}$ ~8 min) (Mayor *et al*., 1998), thereby accumulating inside cells for much longer than other components of the recycling membrane. The rate-limiting step in endocytic recycling may occur in either the GEECs or the REC, with different implications for the mechanism of endocytic trafficking of GPI-APs. If the rate-limiting step in recycling is exit from GEECs, this would suggest that the slower recycling of GPI-APs to the plasma membrane is a result of the characteristic trafficking property of the GEECs. On the other hand, if exit from REC is rate limiting, then GPI-APs would have to be sorted/segregated from recycling receptors and other membrane components in the REC.

Essential functions of many GPI-APs are likely to be mediated by endocytic retention. For example, folate uptake via the human folate receptor (FR-GPI) is severely impaired in cholesterol-depleted cells (Chang *et al*., 1992) in which FR-GPI is no longer retained in endosomes (Mayor *et al*., 1998). Folate uptake via FR-GPI is also severely impaired upon depletion of sphingolipids by treatment of cells with Fumonisin B_1 (FB_1), a fungal metabolite from *Fusarium moniliforme*, which inhibits sphingosine *N*-acyl-transferase (Stevens and Tang, 1997). It is likely that sphingolipid levels in cells could also influence endocytic retention of GPI-APs in a manner similar to cholesterol.

In this report, we have used monovalent fluorescent ligands to compare the endocytic route and kinetics of

trafficking of GPI-APs and FR isoforms lacking GPI anchors, with a marker of the clathrin-pit-mediated pathway, TfR. We have identified the site at which endocytic retention of GPI-AP takes place: retention occurs in the REC and requires the presence of the GPI anchor. We have shown previously that cholesterol depletion abolishes endocytic retention of GPI-APs (Mayor *et al*., 1998), and here we have examined the role of sphingolipids in the endocytic recycling of GPI-APs. We show that sphingolipids are necessary for the retention of GPI-APs in the REC; depletion of sphingolipids dramatically increases the rate of recycling of GPI-APs from the REC. These results, taken together, strongly suggest that the endocytic retention of GPI-APs is mediated by cholesterol and sphingolipid-dependent entities called 'rafts' (Simons and Ikonen, 1997).

Results

GPI anchoring leads to endocytic retention in the pericentriolar REC

FR-GPI and GPI-anchored decay accelerating factor (DAF) are extensively co-localized with TfR in the REC as previously observed by horseradish peroxidase (HRP)-mediated quenching and immunoelectron microscopy (EM) methodologies, respectively (Mayor *et al*., 1998). Despite this extensive co-localization, a significant fraction of the internalized GPI-AP pool is consistently separate from TfR (Mayor *et al*., 1998). Accumulation of GPI-APs in GEECs (S.Sabharanjak and S.Mayor, in preparation) provides an explanation for the lack of co-localization of a fraction of internalized GPI-APs with TfR-containing endosomes (Mayor *et al*., 1998). This fraction of GPI-APs co-localizes with fluid-phase markers but not with Tf or low-density lipoproteins (LDLs) that are internalized into sorting endosomes (data not shown).

To identify the rate-limiting step in the recycling of GPI-APs to the cell surface, we measured the rates of exit of GPI-APs from the GEECs and the REC (Figure 1). As described by Mayor *et al*. (1998), the rate of approach to steady state is a measure of the rate of exit from a kinetically defined compartment. Therefore, we measured the rate of approach to steady state of internalized FR-GPI ligand, N^{α}-pteroyl-N^{ε}-(4′-rhodamine-thiocarbamoyl)-L-lysine (PLR), in the REC and the GEECs, identified as described in Materials and methods. The amount of FR-GPI, as measured by the extent of PLR fluorescence in the peripheral GEECs (Figure 1A and B; arrows), remained unchanged between the 20 and 60 min time points, whereas there was a dramatic increase in PLR fluorescence in the REC between the 20 and 60 min time points (Figure 1A and B; arrowheads). Kinetic analyses of these data show that FR-GPI reaches steady state in the GEECs much earlier than in the REC (Figure 1E). The kinetics of exit of FR-GPI from the GEECs and the REC are well described as a first-order process (Figure 1E, lines represent the theoretical fit; $R \geqslant 0.98$), although we can not rule out undetected contributions from additional processes. The $t_{1/2}$ of exit from the GEECs is ~13 min (k_e 0.05 min^{-1}) while that from the REC is ~30 min (k_e 0.022 min^{-1}) (Figure 1F). Since the $t_{1/2}$ for recycling of FR-GPI to the cell surface measured in the same experiment is also 30 min (k_e 0.023 min^{-1}; Figure 1F, see also Table II), these

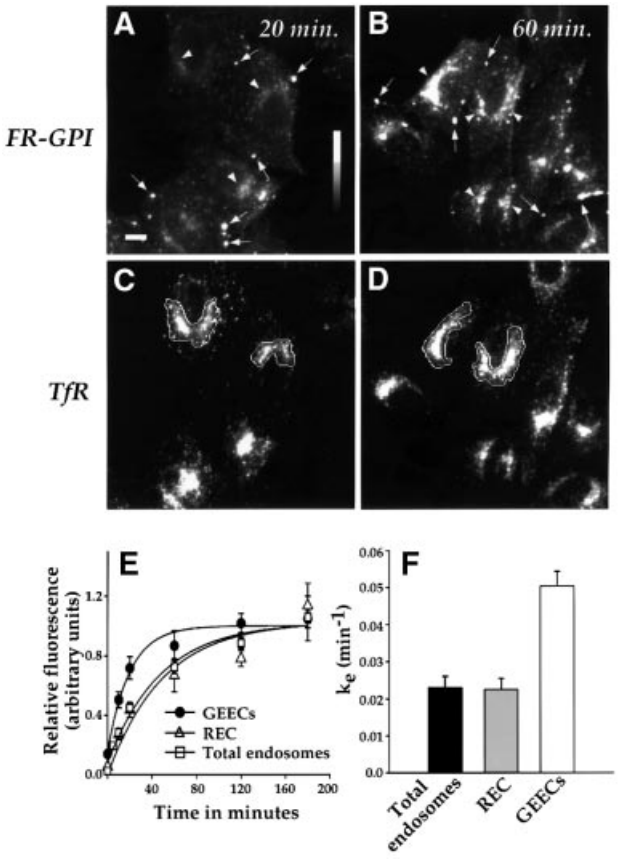

Fig. 1. Trafficking kinetics of FR-GPI measured in endocytic compartments of CHO cells. FRαTb-1 cells were incubated with PLR to determine the extent of accumulation of endocytosed FR-GPI in the peripheral GEECs (arrows) and the pericentriolar REC (arrowheads) after a 20 (**A**) or 60 min (**B**) pulse of the label (see Materials and methods). (A) and (B) show gray-scale intensities of endocytosed PLR normalized to surface FR-GPI expression. The bar shows a gradient of gray-scale intensities with the lowest (black) at the bottom of the bar to the highest (white) at the top of the bar. (**C** and **D**) REC-localized Cy5-Tf images of the same cells in (A) and (B), obtained as described in Materials and methods. The REC is marked with a white boundary for two representative cells. Scale bar represents 5 μm. (**E**) Change in surface receptor-normalized fluorescence in intracellular compartments plotted against time of incubation for the total endosomal FR-GPI (open squares), FR-GPI in REC (open triangle) and FR-GPI in GEECs (filled circles). The lines represent the best fit for the data points using the kinetic equation described in Materials and methods. Note that GEECs reach a steady state of PLR labeling much more quickly than the REC or the total endosomal receptors. (**F**) Rate constant of exit (k_e) from the indicated compartments.

data show that the rate-limiting step in the recycling of the internalized GPI-APs is their exit from REC. The slow rate of recycling of GPI-APs results in the accumulation of GPI-APs in the REC for extended times, confirming that GPI-APs are sorted/segregated from other recycling membrane components in the REC.

To examine whether this manifestation of endocytic sorting, namely retention in the REC, is mediated by the presence of the GPI anchor, we compared the extent of accumulation of FR-GPI and two isoforms of FR, FR-TM and FR-TA, lacking the GPI anchor. FR-TM has the folate-binding portion fused to the transmembrane region of the Fc receptor and the cytoplasmic tail of the LDL receptor (Varma and Mayor, 1998), and FR-TA bears the same transmembrane and cytoplasmic tail region as

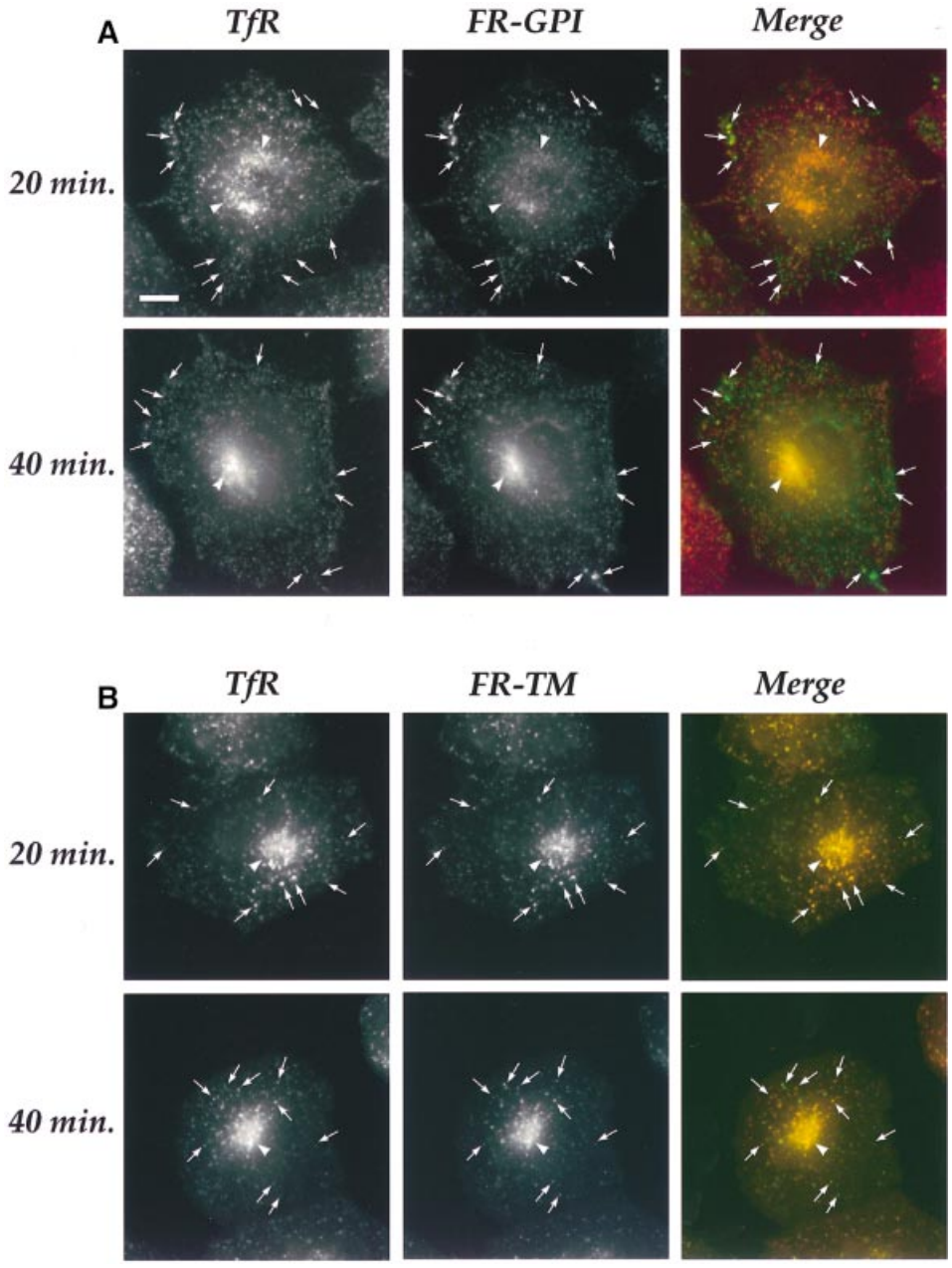

Fig. 2. Retention of FR-GPI in the REC requires the GPI anchor. FRαTb-1 (**A**) and FR-TMTb-1 (**B**) cells expressing FR-GPI and FR-TM, respectively, were labeled with PLR and Cy5-Tf for the indicated times and imaged using a wide-field microscope. Pseudo-colored merges of PLR (encoded green) and Cy5-Tf (encoded red) images are shown in the extreme right-hand panel ('Merge'). Images at the two time points in (A) and (B) were selected for matching total TfR expression and the endosomal PLR fluorescence was normalized to surface receptor expression. Note the change in PLR fluorescence in the REC (arrowheads) compared with that in peripheral endosomes in (A) (arrows indicate GEECs) or (B) (arrows indicate sorting endosomes) between the 20 and 40 min time points. Scale bar represents 10 μm.

FR-TM but has three critical tyrosines mutated to alanine, rendering it incapable of being recognized by a cytoplasmic sorting machinery (Matter *et al*., 1993). As described above and shown in Figure 2A, FR-GPI continues to accumulate in TfR-containing REC, while the distribution and amount of internalized transferrin (Tf) bound to TfR has already reached a steady state by 20 min (Mayor *et al*., 1993). On the other hand, FR-TM and FR-TA traffic in a morphologically and kinetically identical manner to TfR; there is no change in the amount and distribution of internalized PLR bound to FR-TM (Figure 2B) and FR-TA (data not shown) with respect to endocytosed Tf bound to its receptor. These data show that retention in the REC in preference to other recycling membrane proteins requires the presence of a GPI anchor.

Endocytic retention is relieved upon depletion of sphingolipids

To determine whether sphingolipids play a role in the endocytic retention of GPI-APs, we used a well characterized sphingolipid synthesis inhibitor, FB_1, which inhibits sphingosine *N*-acyltransferase (Figure 3; Wang *et al*.,

Table I. Lipid analysis of FB_1-treated cells

Lipid	Lipid content, nmol/mg protein (mean ± SD)		
	Control	FB_1	FB_1 + C_6-ceramide
Cholesterol	72.6 ± 10.8	76.1 ± 6.7	69.3 ± 19.4
Triacylglycerol	55.7 ± 20.0	51.1 ± 34.8	55.1 ± 28.3
Phosphatidylcholine	65.5 ± 37.0	66.6 ± 19.6	93.1 ± 46.5
Phosphatidylethanolamine	50.3 ± 1.1	54.5 ± 9.0	21.0 ± 0.8
Phosphatidylserine	3.7 ± 1.6	2.9 ± 0.8	6.3 ± 0.1
Phosphatidylinositol	7.4 ± 4.3	7.7 ± 4.2	12.8 ± 1.7
Sphingomyelin	15.1 ± 1.6	5.5 ± 1.3	8.4 ± 2.9
Ceramides	16.4 ± 2.4	10.1 ± 2.3	21.7 ± 7.3
Galactosylceramide	6.8 ± 1.5	3.5 ± 0.4	8.3 ± 1.1
Sulfatides	3.2 ± 1.0	2.2 ± 0.7	3.5 ± 0.3

The lipid composition of FRαTb-1 cells grown in medium supplemented with the indicated chemicals was measured as described in Materials and methods. Results are the mean of three separate analyses.

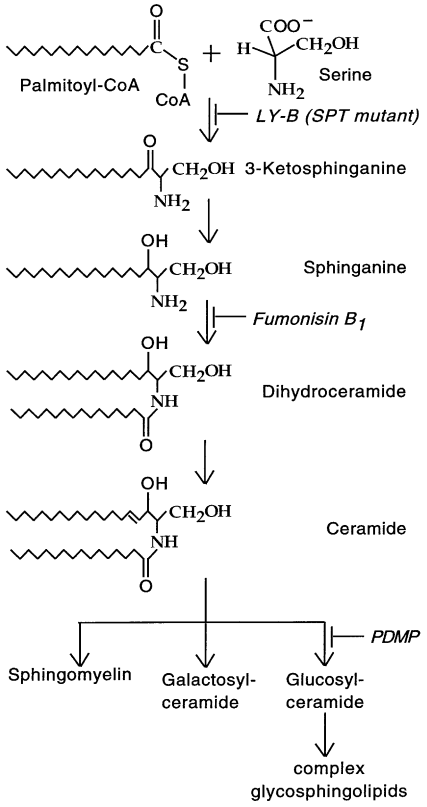

Fig. 3. Schematic of the sphingolipid biosynthesis pathway. The sites of action of the various sphingolipid inhibitors used in this study and the location of the sphingolipid synthesis block in the mutant cell line, LY-B, are indicated by italic text.

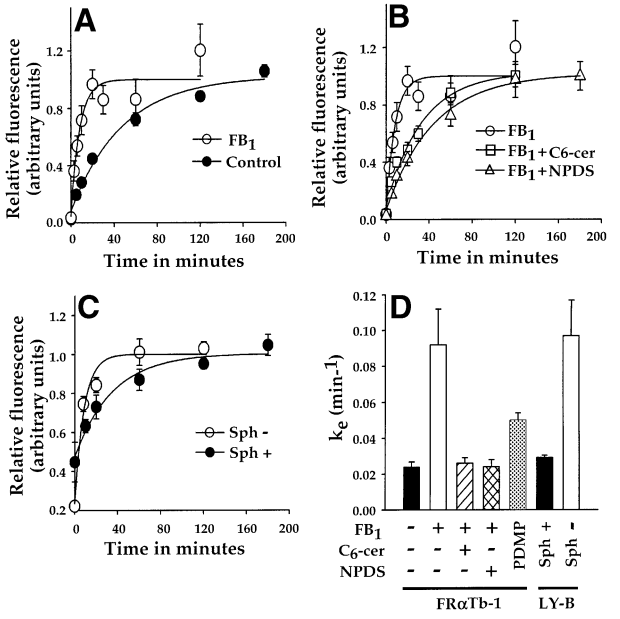

Fig. 4. Sphingolipid depletion increases the rate of recycling of FR-GPI. Fluorescence associated with internalized FR-GPI bound to PLF at indicated times was normalized to surface receptor levels and plotted against time in untreated (control; filled circles) and FB_1-treated (open circles) FRαTb-1 cells (**A** and **B**) and in FB_1-treated FRαTb-1 cells supplemented with exogenous *N*-hexanoyl-D-sphingosine (C_6-cer; open squares) and *N*-palmitoyl-DL-*erythro*-dihydrosphingosine (NPDS; open triangles). Fluorescence associated with internalized PLF bound to FR-GPI at the indicated times was normalized to surface receptor levels and plotted against time in the FR-GPI-expressing LY-B cell line (**C**) grown in sphingolipid-deficient (Sph–; open circles) or sphingolipid-sufficient medium (Sph+; filled circles). The solid lines in (A)–(C) are the best fit for the data points using the kinetic equation described in Materials and methods. (**D**) Rate constants of FR-GPI recycling (k_e) under various treatment conditions. Data are derived from two to six independent experiments for each rate constant determination.

1991; Mays *et al.*, 1995; Stevens and Tang, 1997), to alter sphingolipid levels in cells. FB_1 treatment does not affect cell viability, and lipid analyses of FB_1-treated cells show that there is a reduction in the amount of all major sphingolipid classes without affecting cholesterol levels relative to the untreated controls (Table I). Growing FRαTb-1 cells in the presence of FB_1 resulted in the loss of endocytic retention of FR-GPI (Figure 4A; compare filled and open circles); FR-GPI was recycled to the cell surface at a rate similar to the rate of TfR recycling ($t_{1/2}$ ~6–8 min), without significantly altering its rate of internalization (Table II). Addition of short-chain ceramide, *N*-hexanoyl-D-sphingosine (C_6-ceramide), to FB_1-treated cells in the continuous presence of FB_1 restored the rate of FR-GPI recycling to control levels (Figure 4B; open squares), along with a restoration of sphingolipid levels (Table I).

FB_1 treatment leads to a build-up of sphinganines with a concomitant decrease in ceramide levels (Wang *et al*., 1991; see also Figure 3). Either of these changes could affect signal transduction pathways in cells (Hannun, 1994) leading to an alteration in the kinetics of endocytic processes (Chen *et al*., 1995). Therefore, we used a different drug, D-threo-1-phenyl-2-decanoylamino-3-morpholino-1-propanol (PDMP), which specifically blocks synthesis of a large class of sphingolipids, the glycosphingolipids (Inokuchi and Radin, 1987; Inokuchi *et al*., 1990), resulting in the accumulation of a different set of sphingolipid precursors from that found after FB_1 treatment (Felding-Habermann *et al*., 1990). PDMP treatment also leads to acceleration in the rate of FR-GPI recycling (Figure 4D and Table II). In another approach we tested whether the rate of FR-GPI recycling was restored to control levels in FB_1-treated cells supplemented with a sphingolipid, *N*-palmitoyl-DL-erythro-dihydrosphingosine (NPDS). The naturally occurring *erythro* isomers of dihydroceramides or their metabolites are incapable of mediating signaling activity in cells (Bielawska *et al*., 1993; Hannun, 1994; Chen *et al*., 1995). NPDS restores the rate of FR-GPI recycling to that in control cells (Figure 4B; open triangles). These data suggest that sphingolipid signaling is unlikely to be involved in regulation of endocytic retention of FR-GPI. However, since sphingolipid intermediates involved in signaling may remain uncharacterized, we can not rule out this possibility altogether.

To rule out further that the loss in endocytic retention of FR-GPI is due to secondary effects of using sphingolipid-depleting drugs, and that the restoration of retention is a result of uncharacterized signaling properties of exogenous sphingolipid analogs, we examined the recycling of FR-GPI in a cell line, LY-B, mutant for the serine palmitoyl transferase enzyme (Hanada *et al*., 1998; see Figure 3). LY-B cells do not accumulate any known signaling-competent sphingolipid precursors, as the block is in the first step of sphingolipid biosynthesis. These cells are unable to make the sphingoid base from endogenous sources, and therefore rely on serum-derived lipids to supplement their sphingolipid pools (Hanada *et al*., 1998). Growing cells in sphingolipid-deficient medium for 48 h leads to sphingolipid levels that are 85% lower than in wild-type cells or cells supplied with exogenous sources of sphingolipid, without affecting cell viability or the content of other major phospholipids (Hanada *et al*., 1998) and cholesterol (Fukasawa *et al*., 2000). The rates of FR-GPI recycling in sphingolipid-replete and sphingolipid-deficient conditions were measured in LY-B cell lines expressing FR-GPI. In cells grown under sphingolipid-deficient conditions, recycling of FR-GPI occurred with a $t_{1/2}$ of 6–8 min, as compared with 27 min in cells grown under conditions that restore normal levels of the lipid (Figure 4C and D). In contrast, the change in the rate of FR-GPI internalization in LY-B cells was relatively insignificant upon sphingolipid depletion: cells depleted of sphingolipids internalized FR-GPI ~1.3-fold more quickly than replete cells. Thus, the loss of endocytic retention of FR-GPI is not due to secondary effects of the drug treatments, and its restoration by addition of exogenous lipids is unlikely to be due to activation of signaling pathways.

To test whether sphingolipid depletion affects recycling of other GPI-APs, we determined the rate of DAF recycling in an FB_1-treated DAF-expressing CHO cell line, DAFTb-1 (Mayor *et al*., 1998). The rate of DAF recycling was accelerated upon treatment with FB_1 without substantially affecting the rate of internalization of DAF (Figure 5; Table II), confirming that the effect of sphingolipid depletion on endocytic retention of FR-GPI is not specific to the type of GPI-AP molecule being studied.

To ensure that FB_1 treatment or addition of exogenous ceramides to FB_1-treated cells did not result in any qualitative alteration in the endocytic pathway of the FR-GPI, we analyzed the co-localization of endocytosed FR-GPI with internalized TfR. Figure 6 shows that endocytosed FR-GPI and TfR were extensively co-localized in the REC in untreated (A and B), FB_1-treated (C and D) or C_6-ceramide-replenished cells (E and F). PDMP treatment or growth of the LY-B cell line under conditions of sphingolipid depletion did not affect co-localization of FR-GPI and TfR in the REC either (data not shown). The majority of internalized FR-GPI and TfR were co-localized in the REC, showing that upon alteration of sphingolipid levels, exit from the REC remains the rate-limiting step in recycling. These data together show that reduction in sphingolipid levels results in the loss of endocytic retention of GPI-APs in the REC; replenishment of sphingolipids results in a restoration of endocytic retention.

Sphingolipid depletion does not affect recycling of transferrin receptors

To test whether the defect in recycling of GPI-APs observed upon sphingolipid depletion is specific to GPI-APs or is a result of a generalized acceleration in recycling rates of all proteins from the REC, we measured the recycling kinetics of wild-type human TfR and a C-terminally truncated TfR (δ3–59TfR) that lacks the clathrin internalization motif. The rates of TfR and δ3–59TfR recycling were not affected by treatment with FB_1 (Figure 7A). The rate of recycling of endogenous hamster TfR in LY-B cells grown in sphingolipid-deficient medium was the same as that in sphingolipid-replete medium (Figure 7B); the rate constants measured are similar to those of the human TfR in FRαTb-1 and δ3–59TfR in δ3–59TRVb cells. These data show that sphingolipid depletion does not lead to a generalized increase in the exit rate of proteins from the REC, since neither those that interact with clathrin coats (TfR) nor those that do not (δ3–59TfR) have altered recycling kinetics. Furthermore, the extent and distribution of the TfR in REC were also unaltered (Figure 6). Thus, sphingolipid depletion specifically abolishes the endocytic retention of GPI-APs in the REC, and does not have a non-specific effect on the kinetics or morphology of the endocytic pathway of other proteins.

Discussion

GPI-APs are delivered to endocytic compartments (GEECs) distinct from those containing molecules endocytosed via the clathrin-mediated pathway. Eventually, GPI-APs are transported to the REC (Mayor *et al*., 1998). Thus, the GPI-AP trafficking pathway merges with the

clathrin pathway at the REC, providing two sites wherein GPI-APs may be retained inside the cell, namely GEECs and REC. In this report we show that the rate-limiting step in the recycling of endocytosed GPI-APs to the cell surface is their exit from the REC. These data are consistent with the co-localization of a large fraction of the endocytosed GPI-AP at steady state in the REC with other membrane components, including the TfR (Mayor *et al*., 1998). Thus, given the differential rates of exit of GPI-APs compared with other membrane components from the REC, GPI-APs must be segregated/sorted in this compartment.

In the secretory pathway, GPI-APs are trafficked from the endoplasmic reticulum (ER) to the Golgi via distinct vesicles (Muniz *et al*., 2000). The requirement for the GPI anchor for endocytic retention and the observation that the recycling of another GPI-AP, DAF, is unaffected by treatment with a weak base, primaquine, whereas the recycling of other transmembrane receptors is inhibited by this treatment (Keller *et al*., 1992), strongly suggest that

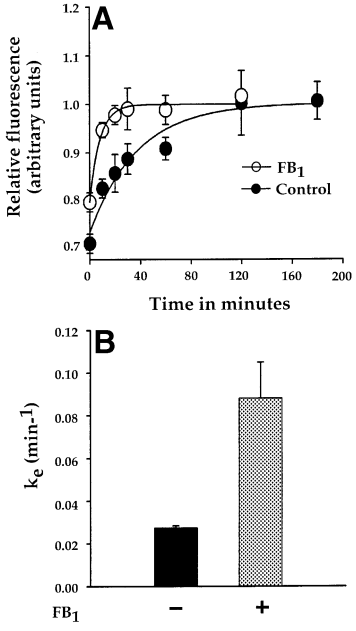

Fig. 5. Rate of recycling of DAF in sphingolipid-depleted cells. (**A**) DAF-associated fluorescence intensity at the indicated times was normalized to surface receptors and plotted against time in untreated (control; filled circles) and FB_1-treated (FB_1; open circles) cells. The solid lines represent the best fit for the data points using the kinetic equation described in Materials and methods. (**B**) Rate constants for DAF recycling in treated and untreated cells.

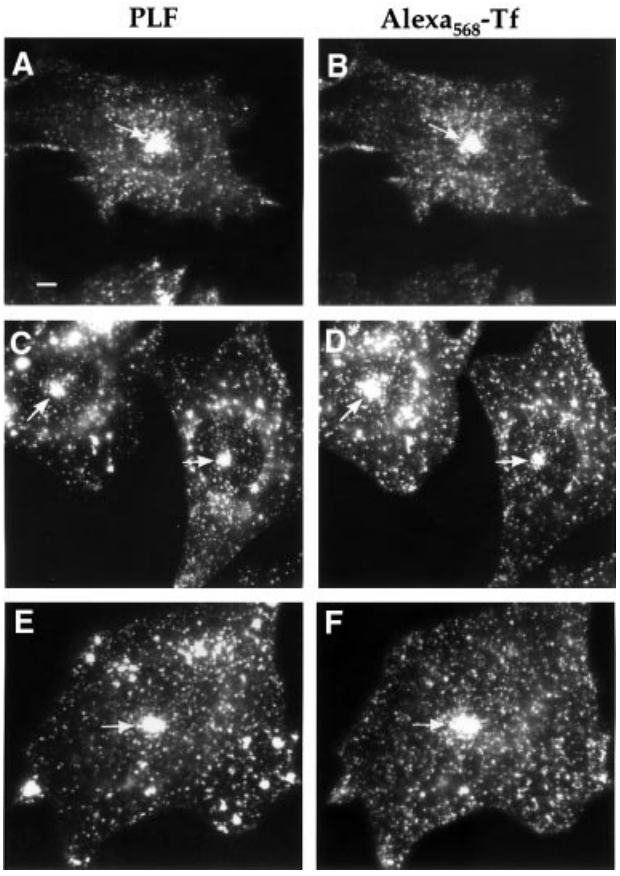

Fig. 6. Endocytic pathway of FR-GPI and TfR in sphingolipid-depleted cells. FRαTb-1 cells were incubated with PLF and $Alexa_{568}$-Tf to steady state, and images of FR-GPI (**A**, **C** and **E**) and TfR (**B**, **D** and **F**) were collected using a wide-field microscope for untreated (A and B), FB_1-treated (C and D) and C_6-ceramide-replenished FB_1-treated cells (E and F). Note that the majority of the intracellular FR-GPI is extensively co-localized with TfR in the REC (arrows). Scale bar represents 10 μm.

Table II. Effect of sphingolipid depletion on the kinetics of GPI-AP trafficking

Cell line	Membrane marker	Treatment	R_i/R_s[a]	k_e, min^{-1} (SD)[b]	k_i, min^{-1} (variance)[c]
FRαTb-1	FR-GPI	–	0.8 (0.04)	0.0237 (0.003)	0.019 (0.003)
FRαTb-1	FR-GPI	FB_1	0.36 (0.038)	0.092 (0.02)	0.033 (0.008)
FRαTb-1	FR-GPI	FB_1 + C_6-ceramide	0.5 (0.04)	0.026 (0.003)	0.013 (0.002)
FRαTb-1	FR-GPI	FB_1 + NPDS	0.42 (0.02)	0.024 (0.004)	0.01 (0.002)
DAFTb-1	DAF	–	0.66 (0.1)	0.0273 (0.001)	0.018 (0.003)
DAFTb-1	DAF	FB_1	0.31 (0.03)	0.088 (0.017)	0.027 (0.006)
FRαTb-1	FR-GPI	PDMP	ND	0.05 (0.004)	–
FRαTb-1	FR-GPI	Compactin[d]	0.41 (0.025)[d]	0.075 (0.015)[d]	0.03 (0.001)[d]
LY-B	FR-GPI	FBS	ND	0.029 (0.0014)	–
LY-B	FR-GPI	Nutridoma	ND	0.097 (0.02)	–

ND, not determined. The data are mean (SD) from at least two independent experiments.
[a]Internal to surface receptor distribution at steady state, determined as described in Materials and methods.
[b]Rate of recycling, determined as described in Materials and methods.
[c]Rate of internalization [$k_e \times (R_i/R_s)$].
[d]Data from Mayor *et al*. (1998).

GPI-APs may exit the REC via distinct vesicular or tubular carriers. Regardless of the mode of exit from the REC, the ability of the GPI anchor to retain proteins in this compartment reveals an important function of this ubiquitous post-translational modification.

The GPI anchor attaches proteins to the exoplasmic (or luminal) leaflet of the cell membrane. It has been suggested, therefore, that apical sorting and transmembrane signaling by different GPI-APs occur by their association with putative cholesterol- and sphingolipid-enriched sorting platforms or 'rafts' involved in a variety of sorting and signaling functions (Simons and Ikonen, 1997). Apical transport is affected by depletion of cholesterol (Hannan and Edidin, 1996) and sphingolipids (Mays *et al*., 1995), and cholesterol depletion severely affects signaling in lymphocytes (Stulnig *et al*., 1997), consistent with this hypothesis. Cholesterol depletion abolishes endocytic retention of GPI-APs without altering the rate-limiting step and the compartment involved in recycling (Mayor *et al*., 1998). The results presented here show that sphingolipids are likely to play a structural rather than signaling role in the endocytic retention of GPI-APs. Therefore, both cholesterol and sphingolipid depletion serve to abrogate endocytic retention independently, strongly implicating a raft-based mechanism for segregation of GPI-APs in the REC.

Although the segregation of cholesterol- and sphingolipid-enriched regions in artificial membranes is well established (for review see Welti and Glaser, 1994; Brown and London, 1998b; Rietveld and Simons, 1998), the detection of rafts in cell membranes has been the subject of intense controversy (Mayor *et al*., 1994; Edidin, 1997; Maxfield and Mayor, 1997; Jacobson and Dietrich, 1999). Single particle tracking (SPT) studies on GPI-APs and potentially raft-associated lipids have revealed differently sized regions of confined motion (Jacobson and Dietrich, 1999; Pralle *et al*., 2000; Schutz *et al*., 2000). Fluorescence resonance energy transfer (FRET) methodology (Varma and Mayor, 1998) and classical chemical cross-linking techniques (Friedrichson and Kurzchalia, 1998) have demonstrated that at least a fraction of GPI-APs are present in small clusters at the surface of living cells. However, experiments using different FRET methodology have not detected these structures (Kenworthy and Edidin, 1998; Kenworthy *et al*., 2000). The role of sphingolipids in the organization of GPI-APs in rafts in cell membranes has not been explored using these methods.

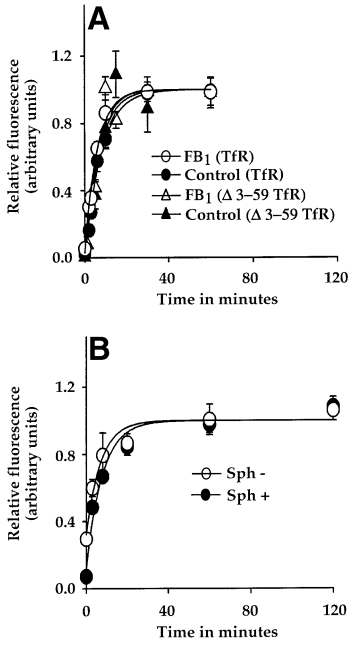

Fig. 7. Sphingolipid depletion does not affect the rate of TfR recycling. (**A**) Internalized Cy3-Tf fluorescence bound to TfR (circles) or δ3–59TfR (triangles) at indicated times was normalized to surface receptor expression and plotted against time in untreated (control; filled symbols) and FB_1-treated (FB_1; open symbols) cells, in FRαTb-1 (TfR) and δ3–59TRVb (δ3–59TfR) cells, respectively. (**B**) Internalized Cy5-Tf fluorescence bound to TfR at the indicated times was normalized to surface receptor expression and plotted against time in LY-B cells grown in sphingolipid-deficient (open circle; Sph–) or sphingolipid-sufficient medium (filled circle; Sph+). The solid lines in (A) and (B) represent the best fit for the data points using the kinetic equation described in Materials and methods.

Other means for studying 'rafts' have been based on the inability of non-ionic detergents to solubilize lipids and proteins capable of associating with liquid-ordered regions of the membrane (Harder and Simons, 1997; Brown and London, 1998b). Detergent-resistant membranes (DRMs) consisting of cholesterol, sphingolipids, GPI-APs, influenza virus hemagglutinin antigen (HA) and other components have been equated with rafts involved in sorting processes (Fiedler *et al*., 1993; Keller and Simons, 1997; Simons and Ikonen, 1997; Brown and London, 1998a). However, studies on the apical targeting of mutant forms of HA with alterations in the transmembrane region, and GPI-anchored rat growth hormone chimeras, have shown that association with DRMs is not sufficient for apical delivery (Lin *et al*., 1998; Benting *et al*., 1999). Sphingolipid depletion did not alter the Triton X-100 solubility characteristics of transfected GPI-APs in Fisher rat thyroid cells, but altered the apical and basolateral sorting of these proteins (Lipardi *et al*., 2000). These observations question the relationship between DRMs and sorting-competent rafts. Thus, in the absence of convincing biochemical and biophysical evidence, the ability of cholesterol and sphingolipid depletion to perturb the sorting propensity of GPI-APs in the REC and Golgi (Mays *et al*., 1995; Hannan and Edidin, 1996; Lipardi *et al*., 2000) is the strongest evidence for the involvement of rafts in cellular sorting functions.

A simple mechanism for sorting/retention of proteins in intracellular trafficking processes appears to be the formation of large aggregates in the membrane. Marsh *et al*. (1995) have shown that stable-cross-linked TfRs, independent of their clathrin-binding motif, were retained in the REC if the cross-linked species contained >10 monomers. Recently, Rivera *et al*. (2000) have demonstrated that retention of proteins in the ER is maintained by regulated aggregation. Therefore, it is likely that functional GPI-AP-containing rafts built by cholesterol and sphingolipids may be retained in endosomes by similar principles; cholesterol and sphingolipid depletion may alter the size and structure of the GPI-AP structures, abolishing their lateral segregation/sorting in the membrane.

Endocytic retention of GPI-APs is likely to be physiologically relevant. The replacement of the GPI anchor with

a transmembrane proteinaceous anchor leads to loss of endocytic retention of FR-GPI and concomitantly severely impairs folate uptake (Ritter *et al*., 1995). Replacement of the GPI anchor on the cellular prion protein also disrupts scrapie formation in acidic endosomes (Taraboulos *et al*., 1995). Together with the impairment of folate uptake and scrapie formation upon cholesterol depletion (Chang *et al*., 1992; Taraboulos *et al*., 1995), these data strongly suggest that endocytic retention via GPI anchoring has physiological consequences. It is likely that rafts in the REC are the sites where the folate receptor may be in functional synergy with the anion carriers necessary for transport of folate across the membrane (Kamen *et al*., 1991). In the case of scrapie formation, endocytic retention via rafts could lead to sufficient concentration of prion proteins in the plane of the membrane of an acidic organelle for long enough to promote conversion. The cholesterol- and sphingolipid-dependent structural organization of GPI-APs in cell membranes, therefore, warrant further experimentation.

Materials and methods

Materials

Fluorescent derivatives of folic acid, N^{α}-pteroyl-N^{ε}-(4′-fluorescein-thiocarbamoyl)-L-lysine (PLF) and PLR were synthesized as described previously (McAlinden *et al*., 1991), except that PLR was synthesized using lissamine rhodamine sulfonyl chloride (Fluka Chemie AG, Buchs, Switzerland) instead of fluorescein isothiocynate. PLR binds saturably to FR isoforms and is resistant to release at pH 5.0, well below the acidic pH of endosomes. Nigericin and all fluorochromes for conjugation, except Cy3 and Cy5, (Amersham Pharmacia Biotech) were obtained from Molecular Probes (Eugene, OR). Tf was purified (Mayor *et al*., 1993) and all protein-based reagents were labeled with fluorophores according to the manufacturer's instructions. LDL was prepared from fetal bovine serum and labeled with 1,1′-dioctadecyl-3,3,3′,3′)-tetramethylindocarbocyanine perchlorate ['DiI', DiIC18(3)] as previously described (Mayor *et al*., 1993). All dichroic mirrors, excitation and emission filters were from Chroma Technology Corp. (Brattleboro, VT). All reagents were obtained from Sigma Chemical Co. (St Louis, MI) unless indicated otherwise. Fetal bovine serum (FBS) was obtained from Life Technologies (Rockville, MD). PDMP was obtained from Matreya, Inc. (Pleasant Gap, PA). PI-PLC (phosphatidylinositol-specific phospholipase C) was a gift from Martin Low (Columbia University, New York, NY) and Ram Vishwakarma (National Institute of Immunology, New Delhi). A mouse monoclonal antibody (mAb) against the human folate receptor, Mov19, was a gift from Centocor Corp. (Malvern, PA). A mouse mAb against human DAF (human anti-CD55) was purchased from PharMingen (San Diego, CA). Anti-human transferrin receptor antibody and Nutridoma-SP were obtained from Boehringer Mannheim (Roche Diagnostics, Mumbai, India).

Cells and cell culture

DAF-, FR-GPI-, FR-TM- and δ3–59TfR-expressing CHO cells (DAFTb-1; FRαTb-1, FR-TM-Tb-1 and δ3–59TRVb cells, respectively) were maintained as described previously (Mayor *et al*., 1998; Varma and Mayor, 1998). FR-GPI-expressing LY-B lines were obtained by transfecting LY-B cells (Hanada *et al*., 1998) with FR-GPI cDNA in plasmid pMEP4 as previously described (Mayor and Maxfield, 1995). Transfected LY-B lines were maintained in folate-free HF-12 supplemented with 5% FBS, 50 μg/ml hygromycin and 100 μg/ml penicillin–streptomycin. cDNA for FR-TA was obtained and transfected into TRVb-1 cells (FR-TA-Tb-1 cells) exactly as described for FR-TM (Varma and Mayor, 1998).

Fluorescent labeling and co-localization studies

All microscopy was carried out on cells grown on poly(D-lysine)-coated 35 mm cover-slip bottom dishes as previously described (Mayor *et al*., 1998). Fluorescent labels were made up to appropriate concentrations in labeling medium (folate-free HF-12, 0.3 mg/ml $NaHCO_3$, 5% dialyzed serum, 15 mM HEPES pH 7.2). Cells were washed in medium 1 (150 mM NaCl, 5 mM KCl, 1 mM $CaCl_2$, 1 mM $MgCl_2$, 20 mM HEPES pH 7.4). Fluorescent folic acid analogs were removed from their receptors by multiple washes with ascorbate buffer (140 mM sodium ascorbate, 65 mM ascorbic acid, 1 mM $CaCl_2$, 1 mM $MgCl_2$ pH 4.5).

Cells expressing FR isoforms were plated in medium containing 5% dialyzed FBS 3 days prior to labeling. Cell surface labeling was carried out by incubation of the cells with the indicated ligands for 1 h at 0°C in labeling medium. Excess label was removed by washing with medium 1 prior to microscopy. Total endosomal receptor labeling was carried out by incubation of cells with indicated ligands for 3 h at 37°C and then the surface receptors were stripped off their ligands by treatment with chilled ascorbate buffer (4 × 15 min at 0°C). This procedure removes >95% of the cell surface receptors without affecting the labeling of the endocytosed receptors. Imaging of cells was carried out in the presence of 10 μM nigericin in a high-potassium buffer (120 mM KCl, 5 mM NaCl, 1 mM $CaCl_2$, 1 mM $MgCl_2$, 20 mM HEPES pH 7.4) to neutralize endosomal pH.

Co-localization studies were carried out by labeling cells with 10 nM PLF and 10 μg/ml Alexa-568-Tf for 3 h at 37°C followed by removal of surface receptors by PI-PLC treatment and imaging on a wide-field system using a 60× objective. Appropriate dichroic and emission filters were used so that there was no detectable cross-over of fluorescence emission for the two fluorophores when imaged singly.

Lipid depletions and repletion

Cells were depleted of sphingolipids by growing them in the presence of 40 μg/ml FB_1 for 64–68 h before labeling. Sphingolipid analogs were added by making 1:1 molar mixtures of lipid with defatted bovine serum albumin. C_6-ceramide and NPDS were added at 1 and 5 μM, respectively, to the FB_1-containing culture medium 12 h before imaging. PDMP treatment was done by growing the cells in 10 μM PDMP in the culture medium for 64–68 h. Sphingolipid depletion in LY-B lines was carried out exactly as previously described (Hanada *et al*., 1998), except that 1% dialyzed Nutridoma was used in the depletion medium. Dialyzed Nutridoma has similar effects on cell growth as Nutridoma (Hanada *et al*., 1998).

Fluorescence imaging, quantification and processing

Fluorescence imaging was carried out using a wide-field imaging system [Nikon Eclipse TE300 or Diaphot TMD equipped with a digital CCD camera with a TEK-512×512 D-series back-illuminated chip (Princeton Instruments, Princeton, NJ)] controlled using Metamorph software. For all experiments 20× (0.75 n.a.) or 60× (1.4 n.a., oil) objectives (Nikon, Japan) were used. Fluorescence images were processed using routines in MetaMorph software following previously described procedures (Mayor *et al*., 1993).

To measure the amount of endocytosed FR-GPI, internalized PLF (or PLR)-fluorescence from individual cells was normalized against surface-bound Cy3-Mov19 (or the second-color folate). In the case of DAF, internalized Cy5-conjugated anti-DAF fluorescence was normalized against surface-bound primary antibody detected via Alexa-488-conjugated goat-anti-mouse secondary antibody. In the case of TfR, internalized Cy5-conjugated Tf fluorescence bound to TfR was normalized against the number of cells in a field or surface receptors detected via Alexa-488- or fluorescein isothiocyanate (FITC)-conjugated secondary antibody against primary antibody bound to surface TfR.

In each experiment, normalized fluorescence was calculated from 12–16 fields from duplicate dishes for each time point, and the weighted mean value and the uncertainty in the mean were determined on a per field basis considering each field (consisting of 5–30 cells) to be an independent event, as previously described (Mayor *et al*., 1993).

Measurement of trafficking rates

In general, the rates of recycling (or exit rates) and internalization were obtained by determining the rates of approach to steady state of labeling in the whole cell (or in the GEECs or REC), under conditions where the cell surface receptors were labeled to saturation at all times in the experiment. The recycling rate, k_e, was determined by fitting the data to a single exponent of the form $f = a + b\,[1 - \exp(-k_e t)]$, using the method of least squares provided in SigmaPlot version 4 (SPSS Inc.). The rate of internalization of FR-GPI or DAF was determined from the first-order steady-state kinetic equation exactly as described in Mayor *et al*. (1993).

Rate of GPI-AP recycling

The rate of recycling of FR-GPI to the cell surface was measured as previously described (Mayor *et al*., 1998), using either of two assays with identical results. In both assays, FR-GPI-expressing cells were incubated

with saturating amounts of the fluorescent ligand for the indicated times at 37°C until a steady state of labeling was reached. Subsequently, in one of the assays (where PLF was used as the fluorescent ligand), Cy3-conjugated Mov19 was used to normalize the amount of surface receptor expression. In the other assay, surface-bound fluorescent ligand (PLF or PLR) was removed with chilled ascorbate buffer and labeled with saturating amounts of the second-color ligand on ice to normalize for surface receptor expression. The rate of DAF recycling was measured exactly as described (Mayor *et al*., 1998), except that complete Cy5-conjugated anti-DAF mouse IgG instead of Fab fragments was used to label the recycled DAF. Identical rates were obtained using intact antibody or Fab (data not shown).

Rate of exit from REC and GEECs

The efflux kinetics of FR-GPI from REC (or the GEECs) were determined using an assay similar to that used for measuring the rate of FR-GPI recycling from the whole cell, except that REC (or GEEC)-associated PLR fluorescence was quantified at each time point. For this purpose, the REC in each cell was identified by co-labeling cells at each time point with a 20 min pulse of Cy5-Tf (10 μg/ml) followed by a 10 min chase in a Cy5-Tf-free medium containing 20 μM deferroxamine. This protocol ensures that Tf label is present mainly in the REC (Presley *et al*., 1993). Surface-bound PLR was removed using chilled ascorbate buffer. The cells were then mildly fixed on ice with 1% paraformaldehyde. The surface receptors were then bound to PLF and normalized for surface receptor expression. The cells were imaged for PLR, PLF and Cy5-Tf using appropriate filters. The REC in the Cy5-Tf image was manually marked using the 'draw region' routine available in Metamorph software, and the PLR fluorescence co-localized with this structure was quantified. The rate of exit of FR-GPI from GEECs was determined from the same experiment by subtracting the REC-associated PLR fluorescence from the total internalized PLR fluorescence. In separate experiments we determined that the PLR fluorescence in peripheral endosomes (not associated with the REC) was co-localized with the fluid-phase marker, FITC-conjugated dextran, but not with endocytosed Tf and LDL (data not shown).

Rate of TfR recycling

The rate of recycling of TfR in FRαTb-1, LY-B and δ3–59TRVb cells was measured as described previously (Mayor *et al*., 1993), except that in LY-B lines expressing endogenous hamster TfR, 20 μg/ml of Tf was used to label the receptors.

Lipid analysis

Lipids were extracted and purified from FRαTb-1 as described (Ariga *et al*., 1988) with a few modifications. Cells (~2.5×10^8) were sequentially extracted as described (Stevens and Tang, 1997). Neutral and acidic lipids were resolved on silica HP-TLC plates that had been pre-run in chloroform–methanol–water (60:35:8, by volume) and heated to 100°C for 30 min. After application of standards and samples, the lipids were resolved by running the HP-TLC plates first in chloroform–methanol–acetic acid–formic acid–water (35:15:6:2:1, by volume) to ~12 cm from the origin, followed by hexane–diethyl ether–acetic acid (65:35:2, by volume) to the top of the plate. The lipids were identified and quantified as described (Brown and Rose, 1992). They were visualized by charring with cupric acetate and identified by co-migration with standards, and quantified by densitometric scanning and comparison with standards (Ariga *et al*., 1988).

Acknowledgements

We thank R.Vishwakarma for synthesizing folic acid analogs, R.Varma for generating human FR-GPI-expressing clones of LY-B, S.Sabharanjak for the FR-TA-expressing cell line, M.Low for a generous gift of PI-PLC, and R.Varma and S.Sabharanjak for their comments on the manuscript. S.M. wishes to thank F.F.Bosphorus and K.Belur for inspiration. S.M. thanks the Human Frontier Science Program, The Wellcome Trust (grant no. 056727/Z/99) and the National Centre for Biological Sciences for support.

References

Ariga,T., Macala,L.J., Saito,M., Margolis,R.K., Greene,L.A., Margolis,R.U. and Yu,R.K. (1988) Lipid composition of PC12 pheochromocytoma cells: characterization of globoside as a major neutral glycolipid. *Biochemistry*, **27**, 52–58.

Bamezai,A., Goldmacher,V.S. and Rock,K.L. (1992) Internalization of glycosyl-phosphatidylinositol (GPI)-anchored lymphocyte proteins. II. GPI-anchored and transmembrane molecules internalize through distinct pathways. *Eur. J. Immunol.*, **22**, 15–21.

Benting,J.H., Rietveld,A.G. and Simons,K. (1999) *N*-Glycans mediate the apical sorting of a GPI-anchored, raft-associated protein in Madin–Darby canine kidney cells. *J. Cell Biol.*, **146**, 313–320.

Bielawska,A., Crane,H.M., Liotta,D., Obeid,L.M. and Hannun,Y.A. (1993) Selectivity of ceramide-mediated biology. Lack of activity of *erythro*-dihydroceramide. *J. Biol. Chem.*, **268**, 26226–26232.

Brown,D.A. and London,E. (1998a) Functions of lipid rafts in biological membranes. *Annu. Rev. Cell. Dev. Biol.*, **14**, 111–136.

Brown,D.A. and London,E. (1998b) Structure and origin of ordered lipid domains in biological membranes. *J. Membr. Biol.*, **164**, 103–114.

Brown,D.A. and Rose,J.K. (1992) Sorting of GPI-anchored proteins to glycolipid-enriched membrane subdomains during transport to the apical cell surface. *Cell*, **68**, 533–544.

Chang,W.J., Rothberg,K.G., Kamen,B.A. and Anderson,R.G. (1992) Lowering the cholesterol content of MA104 cells inhibits receptor-mediated transport of folate. *J. Cell Biol.*, **118**, 63–69.

Chen,C.S., Rosenwald,A.G. and Pagano,R.E. (1995) Ceramide as a modulator of endocytosis. *J. Biol. Chem.*, **270**, 13291–13297.

Edidin,M. (1997) Lipid microdomains in cell surface membranes. *Curr. Opin. Struct. Biol.*, **7**, 528–532.

Felding-Habermann,B., Igarashi,Y., Fenderson,B.A., Park,L.S., Radin,N.S., Inokuchi,J., Strassmann,G., Handa,K. and Hakomori,S. (1990) A ceramide analogue inhibits T cell proliferative response through inhibition of glycosphingolipid synthesis and enhancement of *N*,*N*-dimethylsphingosine synthesis. *Biochemistry*, **29**, 6314–6322.

Ferguson,M.A.J. (1994) What can GPI do for you? *Parasitol. Today*, **10**, 48–52.

Fiedler,K., Kobayashi,T., Kurzchalia,T.V. and Simons,K. (1993) Glycosphingolipid-enriched, detergent-insoluble complexes in protein sorting in epithelial cells. *Biochemistry*, **32**, 6365–6373.

Friedrichson,T. and Kurzchalia,T.V. (1998) Microdomains of GPI-anchored proteins in living cells revealed by crosslinking. *Nature*, **394**, 802–805.

Fukasawa,M., Nishijima,M., Itabe,H., Takano,T. and Hanada,K. (2000) Reduction of sphingomyelin level without accumulation of ceramide in chinese hamster ovary cells affects detergent-resistant membrane domains and enhances cellular cholesterol efflux to methyl-β-cyclodextrin. *J. Biol. Chem.*, **275**, 34028–34034.

Gruenberg,J. and Maxfield,F.R. (1995) Membrane transport in the endocytic pathway. *Curr. Opin. Cell Biol.*, **7**, 552–563.

Hanada,K., Hara,T., Fukasawa,M., Yamaji,A., Umeda,M. and Nishijima,M. (1998) Mammalian cell mutants resistant to a sphingomyelin-directed cytolysin. Genetic and biochemical evidence for complex formation of the LCB1 protein with the LCB2 protein for serine palmitoyltransferase. *J. Biol. Chem.*, **273**, 33787–33794.

Hannan,L.A. and Edidin,M. (1996) Traffic, polarity and detergent solubility of a glycosylphosphatidylinositol-anchored protein after LDL-deprivation of MDCK cells. *J. Cell Biol.*, **133**, 1265–1276.

Hannun,Y.A. (1994) The sphingomyelin cycle and the second messenger function of ceramide. *J. Biol. Chem.*, **269**, 3125–3128.

Harder,T. and Simons,K. (1997) Caveolae, DIGs and the dynamics of sphingolipid–cholesterol microdomains. *Curr. Opin. Cell Biol.*, **9**, 534–542.

Inokuchi,J. and Radin,N.S. (1987) Preparation of the active isomer of 1-phenyl-2-decanoylamino-3-morpholino-1-propanol, inhibitor of murine glucocerebroside synthetase. *J. Lipid Res.*, **28**, 565–571.

Inokuchi,J., Jimbo,M., Momosaki,K., Shimeno,H., Nagamatsu,A. and Radin,N.S. (1990) Inhibition of experimental metastasis of murine Lewis lung carcinoma by an inhibitor of glucosyl ceramide synthase and its possible mechanism of action. *Cancer Res.*, **50**, 6731–6737.

Jacobson,K. and Dietrich,C. (1999) Looking at lipid rafts? *Trends Cell Biol.*, **9**, 87–91.

Johnson,L.S., Dunn,K.W., Pytowski,B. and McGraw,T.E. (1993) Endosome acidification and receptor trafficking: bafilomycin A1 slows receptor externalization by a mechanism involving the receptor's internalization motif. *Mol. Biol. Cell*, **4**, 1251–1266.

Kamen,B.A., Wang,M.T., Streckfuss,A.J., Peryea,X. and Anderson,R.G. (1988) Delivery of folates to the cytoplasm of MA104 cells is mediated by a surface membrane receptor that recycles. *J. Biol. Chem.*, **263**, 13602–13609.

Kamen,B.A., Smith,A.K. and Anderson,R.G. (1991) The folate receptor works in tandem with a probenecid-sensitive carrier in MA104 cells *in vitro*. *J. Clin. Invest.*, **87**, 1442–1449.

Keller,G.A., Siegel,M.W. and Caras,I.W. (1992) Endocytosis of glycophospholipid-anchored and transmembrane forms of CD4 by different endocytic pathways. *EMBO J.*, **11**, 863–874.

Keller,P. and Simons,K. (1997) Post-Golgi biosynthetic trafficking. *J. Cell Sci.*, **110**, 3001–3009.

Kenworthy,A.K. and Edidin,M. (1998) Distribution of a glycosylphosphatidylinositol-anchored protein at the apical surface of MDCK cells examined at a resolution of 100 Å using imaging fluorescence resonance energy transfer. *J. Cell Biol.*, **142**, 69–84.

Kenworthy,A.K., Petranova,N. and Edidin,M. (2000) High-resolution FRET microscopy of cholera toxin B-subunit and GPI-anchored proteins in cell plasma membranes. *Mol. Biol. Cell*, **11**, 1645–1655.

Lin,S., Naim,H.Y., Rodriguez,A.C. and Roth,M.G. (1998) Mutations in the middle of the transmembrane domain reverse the polarity of transport of the influenza virus hemagglutinin in MDCK epithelial cells. *J. Cell Biol.*, **142**, 51–57.

Lipardi,C., Nitsch,L. and Zurzolo,C. (2000) Detergent-insoluble GPI-anchored proteins are apically sorted in Fischer rat thyroid cells, but interference with cholesterol or sphingolipids differentially affects detergent insolubility and apical sorting. *Mol. Biol. Cell*, **11**, 531–542.

Lisanti,M.P., Rodriguez-Boulan,E. and Saltiel,A.R. (1990) Emerging functional roles for the glycosyl-phosphatidylinositol membrane protein anchor. *J. Membr. Biol.*, **117**, 1–10.

Marsh,E.W., Leopold,P.L., Jones,N.L. and Maxfield,F.R. (1995) Oligomerized transferrin receptors are selectively retained by a lumenal sorting signal in a long-lived endocytic recycling compartment. *J. Cell Biol.*, **129**, 1509–1522.

Matter,K., Whitney,J.A., Yamamoto,E.M. and Mellman,I. (1993) Common signals control low density lipoprotein receptor sorting in endosomes and the Golgi complex of MDCK cells. *Cell*, **74**, 1053–1064.

Maxfield,F.R. and Mayor,S. (1997) Cell surface dynamics of GPI-anchored proteins. *Adv. Exp. Med. Biol.*, **419**, 355–364.

Mayor,S. and Maxfield,F.R. (1995) Insolubility and redistribution of GPI-anchored proteins at the cell surface after detergent treatment. *Mol. Biol. Cell*, **6**, 929–944.

Mayor,S., Presley,J.F. and Maxfield,F.R. (1993) Sorting of membrane components from endosomes and subsequent recycling to the cell surface occurs by a bulk flow process. *J. Cell Biol.*, **121**, 1257–1269.

Mayor,S., Rothberg,K.G. and Maxfield,F.R. (1994) Sequestration of GPI-anchored proteins in caveolae triggered by cross-linking. *Science*, **264**, 1948–1951.

Mayor,S., Sabharanjak,S. and Maxfield,F.R. (1998) Cholesterol-dependent retention of GPI-anchored proteins in endosomes. *EMBO J.*, **17**, 4626–4638.

Mays,R.W., Siemers,K.A., Fritz,B.A., Lowe,A.W., van Meer,G. and Nelson,W.J. (1995) Hierarchy of mechanisms involved in generating Na/K-ATPase polarity in MDCK epithelial cells. *J. Cell Biol.*, **130**, 1105–1115.

McAlinden,T.P., Hynes,J.B., Patil,S.A., Westerhof,G.R., Jansen,G., Schornagel,J.H., Kerwar,S.S. and Freisheim,J.H. (1991) Synthesis and biological evaluation of a fluorescent analogue of folic acid. *Biochemistry*, **30**, 5674–5681.

McConville,M.J. and Ferguson,M.A. (1993) The structure, biosynthesis and function of glycosylated phosphatidylinositols in the parasitic protozoa and higher eukaryotes. *Biochem. J.*, **294**, 305–324.

Mukherjee,S., Ghosh,R.N. and Maxfield,F.R. (1997) Endocytosis. *Physiol. Rev.*, **77**, 759–803.

Muniz,M., Nuoffer,C., Hauri,H.P. and Riezman,H. (2000) The Emp24 complex recruits a specific cargo molecule into endoplasmic reticulum-derived vesicles. *J. Cell Biol.*, **148**, 925–930.

Pralle,A., Keller,P., Florin,E., Simons,K. and Horber,J.K. (2000) Sphingolipid–cholesterol rafts diffuse as small entities in the plasma membrane of mammalian cells. *J. Cell Biol.*, **148**, 997–1008.

Presley,J.F., Mayor,S., Dunn,K.W., Johnson,L.S., McGraw,T.E. and Maxfield,F.R. (1993) The End2 mutation in CHO cells slows the exit of transferrin receptors from the recycling compartment but bulk membrane recycling is unaffected. *J. Cell Biol.*, **122**, 1231–1241.

Ricci,V., Galmiche,A., Doye,A., Necchi,V., Solcia,E. and Boquet,P. (2000) High cell sensitivity to *Helicobacter pylori* VacA toxin depends on a GPI-anchored protein and is not blocked by inhibition of the clathrin- mediated pathway of endocytosis. *Mol. Biol. Cell*, **11**, 3897–3909.

Rietveld,A. and Simons,K. (1998) The differential miscibility of lipids as the basis for the formation of functional membrane rafts. *Biochim. Biophys. Acta*, **1376**, 467–479.

Rijnboutt,S., Jansen,G., Posthuma,G., Hynes,J.B., Schornagel,J.H. and Strous,G.J. (1996) Endocytosis of GPI-linked membrane folate receptor-α. *J. Cell Biol.*, **132**, 35–47.

Ritter,T.E., Fajardo,O., Matsue,H. anderson,R.G. and Lacey,S.W. (1995) Folate receptors targeted to clathrin-coated pits cannot regulate vitamin uptake. *Proc. Natl Acad. Sci. USA*, **92**, 3824–3828.

Rivera,V.M. *et al.* (2000) Regulation of protein secretion through controlled aggregation in the endoplasmic reticulum. *Science*, **287**, 826–830.

Robinson,P.J. (1997) Signal transduction via GPI-anchored membrane proteins. *Adv. Exp. Med. Biol.*, **419**, 365–370.

Sabharanjak,S. and Mayor,S. (1999) GPI-anchored proteins are endocytosed via endosomes devoid of transferrin receptors. *Mol. Biol. Cell*, **10**, 399a.

Schutz,G.J., Kada,G., Pastushenko,V.P. and Schindler,H. (2000) Properties of lipid microdomains in a muscle cell membrane visualized by single molecule microscopy. *EMBO J.*, **19**, 892–901.

Simons,K. and Ikonen,E. (1997) Functional rafts in cell membranes. *Nature*, **387**, 569–572.

Skretting,G., Torgersen,M.L., van Deurs,B. and Sandvig,K. (1999) Endocytic mechanisms responsible for uptake of GPI-linked diphtheria toxin receptor. *J. Cell Sci.*, **112**, 3899–3909.

Stevens,V.L. and Tang,J. (1997) Fumonisin B1-induced sphingolipid depletion inhibits vitamin uptake via the glycosylphosphatidylinositol-anchored folate receptor. *J. Biol. Chem.*, **272**, 18020–18025.

Stulnig,T.M., Berger,M., Sigmund,T., Stockinger,H., Horejsi,V. and Waldhausl,W. (1997) Signal transduction via glycosyl phosphatidylinositol-anchored proteins in T cells is inhibited by lowering cellular cholesterol. *J. Biol. Chem.*, **272**, 19242–19247.

Taraboulos,A., Scott,M., Semenov,A., Avrahami,D., Laszlo,L., Prusiner,S.B. and Avraham,D. (1995) Cholesterol depletion and modification of COOH-terminal targeting sequence of the prion protein inhibit formation of the scrapie isoform. *J. Cell Biol.*, **129**, 121–132.

Varma,R. and Mayor,S. (1998) GPI-anchored proteins are organized in submicron domains at the cell surface. *Nature*, **394**, 798–801.

Wang,E., Norred,W.P., Bacon,C.W., Riley,R.T. and Merrill,A.H.,Jr (1991) Inhibition of sphingolipid biosynthesis by fumonisins. Implications for diseases associated with *Fusarium moniliforme*. *J. Biol. Chem.*, **266**, 14486–14490.

Welti,R. and Glaser,M. (1994) Lipid domains in model and biological membranes. *Chem. Phys. Lipids*, **73**, 121–137.

Received November 22, 2000; revised January 23, 2001; accepted February 9, 2001